



Contents lists available at Egyptian Knowledge Bank

Microbial Biosystems

Journal homepage: <http://mb.journals.ekb.eg/>

## Study the association between virulence genes and antibiotic resistance in hypervirulent *Klebsiella pneumoniae* isolates

Najlaa Abd Fouad

Medical Microbiology Department, College of Medicine, Al-Nahrain University, Baghdad, Iraq.



### ARTICLE INFO

#### Article history

Received 14 July 2024

Received revised 26 August 2024

Accepted 4 April 2025

Available online 1 June 2025

#### Corresponding Editors

Hassan, A.

Semesem, H.

#### Keywords

Antibiotic susceptibility patterns,

hypermucoviscous phenotype,

human health,

Iraq,

*Klebsiella pneumoniae*-hypervirulent.

### ABSTRACT

This study investigates differences between classical and hypervirulent *Klebsiella pneumoniae* strains by analyzing virulence genes (*K1*, *K2*, *iutA*, *p-rmpA*, *c-rmpA*, *maga*) and antibiotic resistance. A total of 132 isolates were collected from various sources in six Baghdad hospitals in a cross-sectional study. Hyper-mucoviscosity was determined using the string test, and Vitek2 was used for identification and susceptibility testing. PCR detected virulence genes. Most isolates (46.2%) came from urine, while 0.8% were from umbilical, abscess, and tissue biopsies. Resistance was highest to beta-lactamase and folic acid inhibitors; minocycline showed the lowest resistance. Drug resistance patterns included XDR (30.3%), MDR (22.7%), and PDR (12.1%). Hypervirulent strains accounted for 3.8% of isolates, with 20% showing a hyper-mucoviscous phenotype; 96.2% were classical strains, with 70.1% hyper-mucoviscous. Among hypervirulent strains, 80% showed XDR/MDR patterns versus 64.6% of classical strains. The study found a strong association between hypervirulent strains and resistance. Although only five strains were hypervirulent, 80% showed multiple resistance patterns. Identifying these strains and understanding their resistance profiles is vital for therapy and outbreak control. This study highlights the emerging threat of hypervirulent, extensively drug-resistant *K. pneumoniae* in Iraqi hospitals.

Published by Arab Society for Fungal Conservation

### Introduction

*Klebsiella pneumoniae* is responsible for various human infections (Al Jader & Ibrahim. Mokabel et al. 2024, Hamedo et al. 2025). There are two main pathotypes: classical *K. pneumoniae* (CKp) and hypervirulent *K. pneumoniae* (HvKp). CKp is typically associated with healthcare-acquired infections, while HvKp often causes community-acquired infections, even in healthy individuals (Kocsis, 2023). First identified in Asia, HvKp

has since spread globally, causing a range of serious diseases. Unlike CKp, HvKp has the ability to invade organs such as the liver, eyes, lungs, and central nervous system (Choby et al., 2020).

Molecular studies have shown that HvKp strains possess unique virulence factors, including the regulator of mucoid phenotype A (*rmpA*) and aerobactin (*Aer*), which are often located on a large virulence plasmid absent in most CKp strains (Yang et al., 2022).

\*Corresponding author Email address: abdnajlaa71@gmail.com (Najlaa Abd Fouad)



*Aer* is an iron-chelating siderophore that enhances bacterial growth and pathogenicity. Despite having a lower affinity for iron than other siderophores, *Aer* contributes to approximately 90% of total siderophore production (Russo et al., 2018). This may explain why invasive strains preferentially express *Aer* to acquire iron from host tissues (Holden, 2016). *rmpA/rmpA2* enhances serum resistance by promoting the hypermucoviscous (HMV) phenotype (Russo et al., 2018). While *rmpA* is commonly plasmid-encoded (*p-rmpA*), it also exists in an integrative and conjugative element within the chromosome (*c-rmpA*) (Zhu et al., 2021).

More than 160 capsular types have been identified in *K. pneumoniae*, with *K1* and *K2* serotypes showing higher virulence due to increased resistance to phagocytosis and immune responses (Mendes et al., 2023). Most HvKp isolates belong to these serotypes. Other virulence factors, such as the mucoid-associated gene (*magA*) and iron uptake systems, also contribute to the HvKp phenotype (Ma et al., 2022).

The HMV phenotype, typically detected using the string test (string length  $\geq 5$  mm), is widely used to identify HvKp. However, some CKp strains may also exhibit mucoviscosity, while some HvKp strains may not, indicating that HMV alone cannot reliably distinguish between the two pathotypes (Choby et al., 2020).

*K. pneumoniae* is among the most antibiotic-resistant members of *Enterobacteriaceae*, particularly noted for quinolone resistance (Kaur Gill et al., 2019). Rising resistance to penicillins and cephalosporins is linked to the uncontrolled use of these antibiotics. Chromosome-encoded  $\beta$ -lactamases also contribute to intrinsic resistance (Jomehzadeh et al., 2022). Although hypervirulent strains were historically sensitive to antibiotics (except for intrinsic ampicillin resistance), recent studies report the emergence of MDR and XDR HvKp strains due to plasmid-mediated resistance (Zhu et al., 2021).

This study aims to investigate the prevalence of HvKp strains in Iraq, along with their antibiotic resistance patterns, to improve understanding of the local epidemiological landscape.

## Materials and Methods

### Bacterial Collection and Identification

We conducted a comprehensive analysis of 132 *Klebsiella pneumoniae* isolates obtained from bacteriology laboratories in six government hospitals in Baghdad, Iraq: Ibn Al-Balady Hospital and Medical City Hospitals (Specialized Surgical Hospital, Baghdad Teaching Hospital, Educational Laboratories, and Burns Specialist Hospital). The study was conducted from August 2022 to September 2023 and involved isolates collected from diverse clinical specimens, including

urine, respiratory secretions, blood, wound and burn infections, stool, and other sources. The investigation focused on characterizing the isolates in terms of antimicrobial resistance, presence of virulence genes, and hypermucoviscosity. Of the 132 isolates, 22 recovered from the intensive care unit (ICU) and respiratory care unit (RCU). Identification and antibiotic susceptibility testing were performed using the Vitek2 system.

### Hypermucoviscosity string test

The *K. pneumoniae* phenotype was identified using a standard bacteriological loop to stretch colonies grown on MacConkey agar. A positive hypermucoviscosity phenotype was defined by the formation of a viscous, thread-like string measuring 5 mm or longer. Isolates producing strings shorter than 5 mm were classified as non-hypermucoviscous (Pomakova et al., 2012).

### Identification of virulence-associated genes and capsular serotype-specific genes

DNA was extracted using the Wizard® Genomic DNA Purification Kit (Cat. No. A1120, USA) according to the manufacturer's instructions and stored at  $-20^{\circ}\text{C}$ . Polymerase chain reaction (PCR) was performed using six primer sets (*K1*, *K2*, *p-rmpA*, *c-rmpA*, *magA*, and *iutA*) to identify capsular serotype-specific and virulence-associated genes, differentiating HvKp from CKp.

Each 25  $\mu\text{L}$  PCR master mix consisted of 1X PCR buffer (5X) (Promega, USA), 200  $\mu\text{M}$  dNTPs (Promega, USA), primer concentrations optimized in preliminary runs (Alpha, Canada; see Table 1), and 1.5 units of Taq DNA polymerase (Promega, USA). Nuclease-free water was added to reach 23  $\mu\text{L}$ , and 2  $\mu\text{L}$  of DNA template (100 ng/reaction) was added to each tube. A no-template control (NTC) was prepared by replacing DNA with 2  $\mu\text{L}$  of nuclease-free water.

PCR reactions were run in a thermal cycler (Eppendorf, Germany) under conditions specific to each primer set as shown in table 1 (supplementary). Amplified products were separated via electrophoresis on a 1.5% agarose gel. Ten microliters of each PCR product, the negative control, and a 100 bp DNA ladder (Promega, USA) were loaded. DNA bands were visualized using a UV transilluminator (Consort, Belgium). The presence of bands of expected molecular sizes indicated positive amplification.

### Statistical analysis

Statistical analysis involved calculating percentages and applying Fisher's exact test to evaluate the significance between different study variables. P-values of  $<0.001$ ,  $<0.002$ , and  $<0.003$  were considered highly significant. P-values of  $<0.06$  or  $<0.07$  were considered not

statistically significant. All analyses were performed using SPSS software (version 20).

## Results

### *Distribution of Klebsiella pneumoniae Isolates by Clinical Specimen Types*

Table 2 (supplementary) presents the distribution of 132 *K. pneumoniae* isolates according to the types of clinical specimens. The majority of isolates were obtained from urine (46.2%), followed by respiratory secretions (21.2%) and blood samples (14.4%). These three sources represented the most common specimen types. Isolates were less frequently recovered from abscesses, tissue biopsies, and other sources.

### *Hypermucoviscosity test*

Among the 132 *K. pneumoniae* isolates, 42 (31.8%) exhibited a non-mucoviscous or non-hypermucoid (non-HMV) phenotype, while 90 (66.7%) displayed a hypermucoviscous (HMV) phenotype, as determined by a positive string test (defined as a viscous string >5 mm) as shown in figure 1.

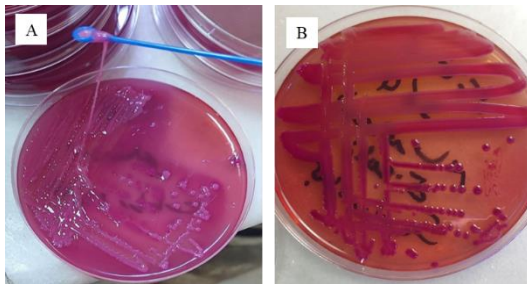


Fig 1. (A) *Klebsiella pneumoniae* colonies exhibiting a hypermucoviscous phenotype, confirmed by a positive string test. (B) Colonies displaying a non-hypermucoviscous phenotype.

### *Antibiotic susceptibility testing of K. pneumoniae isolates*

Antimicrobial susceptibility testing was conducted on all 132 *K. pneumoniae* isolates using a range of antibiotics, including ticarcillin, ticarcillin/clavulanic acid, piperacillin, piperacillin/tazobactam, ceftazidime, cefepime, aztreonam, imipenem, meropenem, amikacin, gentamicin, tobramycin, minocycline, ciprofloxacin, and trimethoprim/sulfamethoxazole. The VITEK-2 compact system (AST A222 cards) was used for testing, and susceptibility interpretations followed the Clinical and Laboratory Standards Institute (CLSI, 2022) guidelines.

### *Analysis of resistance patterns*

The *K. pneumoniae* isolates showed a wide range of resistance patterns. Minocycline and meropenem had the lowest resistance rates. In contrast, resistance was significantly higher than susceptibility for several

antibiotics, including ticarcillin/clavulanic acid, piperacillin, aztreonam, trimethoprim/sulfamethoxazole, piperacillin/tazobactam, and ceftazidime. On the other hand, meropenem, tobramycin, and gentamicin demonstrated higher sensitivity rates. No significant differences in resistance were noted for cefepime or imipenem. Please check table 3 in the supplementary materials.

### *Comparison of resistance profiles*

Figures 2, 3 and table 3 illustrate the differing resistance profiles among general isolates, classical *K. pneumoniae* (CKp), and hypervirulent *K. pneumoniae* (HvKp). Protein synthesis inhibitors (gentamicin, tobramycin, minocycline) exhibited higher resistance in HvKp strains compared to cell wall or folate pathway inhibitors. However, due to the limited number of HvKp and CKp isolates, statistical analysis of resistance differences was not performed.

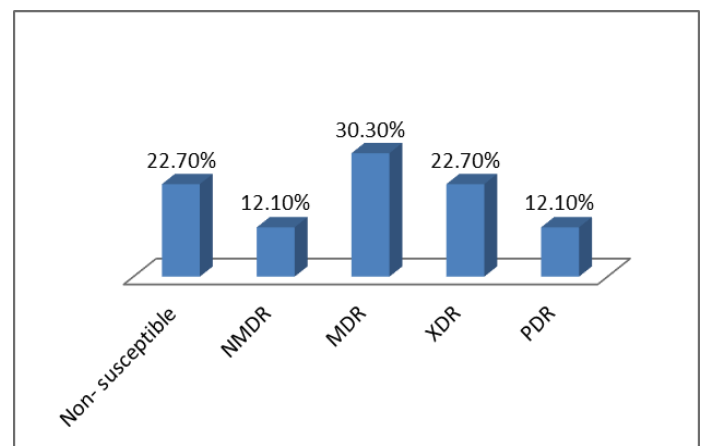
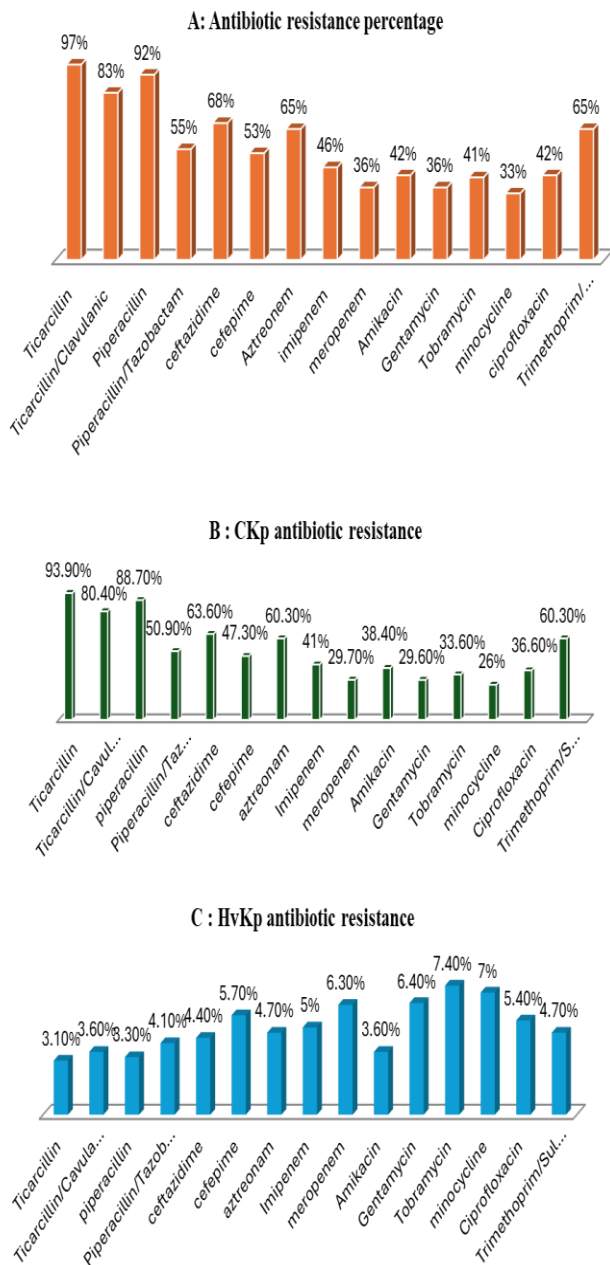


Fig 2. Distribution of antibiotic susceptibility patterns among *K. pneumoniae* isolates.

### *Characterization of multidrug resistance*

The definitions of multidrug-resistant (MDR), extensively drug-resistant (XDR), and pan-drug-resistant (PDR) organisms followed international standards set by the European Centre for Disease Control (ECDC) and the Centers for Disease Control and Prevention (CDC). Non-susceptible isolates were defined as those resistant or not fully susceptible to at least one agent in a given category. Isolates not meeting MDR or XDR criteria were classified as non-multidrug-resistant (NMDR), meaning they were resistant to at least one agent in two categories. The highest resistance was observed in beta-lactamase inhibitors and folate synthesis inhibitors.



**Fig 3.** Percentage resistance to various antibiotic classes in (A) general isolates, (B) CKp, and (C) HvKp.

**MDR, XDR, and PDR rates**

MDR was defined as non-susceptibility to at least one agent in three or more antimicrobial categories. XDR was identified when resistance was observed to all but two or fewer categories, and PDR when resistance occurred across all categories. In this study, 12.1% of isolates were classified as NMDR, 22.7% as MDR, 30.3% as XDR, and 12.1% as PDR. The XDR pattern was the most frequently observed (30.3%), as illustrated in figure 2.

**PCR Amplification of virulence genes in *K. pneumoniae* isolates**

**Capsular serotyping K1 and K2**

PCR amplification was used to detect the K1 and K2 capsular serotypes, which are linked to virulence. Of the 132 isolates, 3 (2.3%) were positive for K1, and 11 (8.3%) were positive for K2. Figures 4 and 5 show the PCR products for K1 and K2, respectively. The remaining 118 isolates (89.4%) were negative for both and were categorized as non-K1/K2.

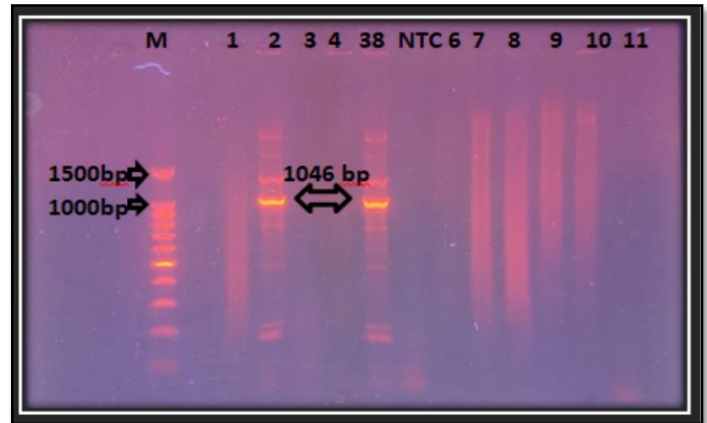


**Fig 4.** PCR amplification of the K1 gene using serotype-specific primers. Electrophoresis was performed using 1.5% agarose gel at 5V/cm for 2 hours. Lanes 1–11 show amplified K1 products (1046 bp). M = molecular size ladder (100 bp); NTC = no template control.

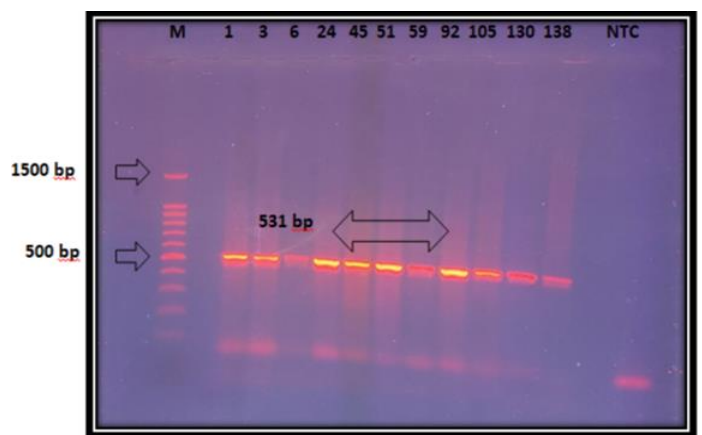


**Fig 5.** Gel electrophoresis of PCR-amplified products from *Klebsiella pneumoniae* K2 strains using serotype-specific primers. A 1.5% agarose gel was run at 5 V/cm for 2 hours. Lanes 1–138 show amplification products of 531 bp, consistent with the K2 serotype. Lane "M" contains a 100 bp molecular size ladder, and the "NTC" lane represents the no-template control, showing no amplification.

### Detection of additional virulence genes

PCR was performed to amplify four additional virulence genes: *iutA*, *c-rmpA*, *magA*, and *P-rmpA*. Of the 132 isolates, 4 (3.0%) were positive for *iutA*, while none tested positive for *c-rmpA* or *magA*. Only one isolate (0.8%) was positive for *P-rmpA*. Figures 6 and 7 show the PCR products for *iutA* and *P-rmpA*, respectively.

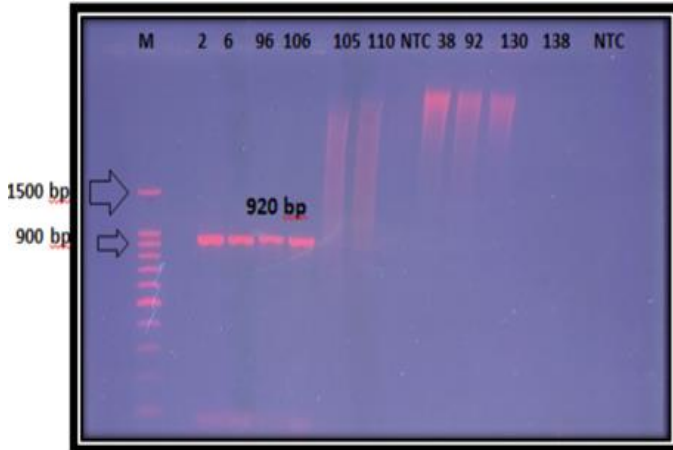


**Fig 6.** Gel electrophoresis of PCR-amplified *iutA* gene using specific primers for *Klebsiella pneumoniae*. Electrophoresis was performed on a 1.5% agarose gel at 5 V/cm for 2 hours. Lanes 2–138 represent the amplified *iutA* gene products (~920 bp) from various strains. M: 100 bp DNA ladder (molecular size marker). NTC: no-template control.

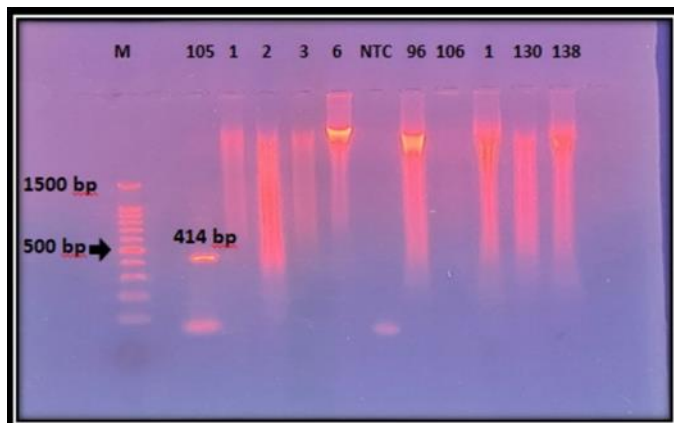


**Fig 7.** Gel electrophoresis of PCR amplified *P-rmpA* by using specific primers of *K. pneumoniae*. The electrophoresis was done with 1.5 % agarose gel at (5V/cm) for 4 hrs, Lane (105-138) No. of strains, amplified products of *P-rmpA* (414) bp, M: molecular size ladder of 100bp. NTC: no template control.

### Characterization of hypervirulent *K. pneumoniae* (HvKp) strains

In the present study, five strains were classified as HvKp: NA2 (Non-HMV/K1/*iutA*), NA6 (Non-HMV/K2/*iutA*), NA96 (HMV/Non-K1/K2/*iutA*), NA105 (Non-HMV/K2/*rmpA*), and NA106 (Non-HMV/Non-K1/K2/*iutA*). These represent 5 out of 132 isolates (3.8%) of the total strain population. The remaining 127 isolates (96.2%) were classified as classical *K. pneumoniae* (CKp).

### Analysis of CKp strains

The CKp strains showed the following phenotype/capsular combinations:

NA1 (Non-HMV/K2), NA3 (Non-HMV/K2), NA24 (HMV/K2), NA38 (HMV/K1), NA45 (HMV/K2), NA51 (HMV/K2), NA59 (HMV/K2), NA92 (HMV/K2), NA110 (HMV/K1), NA130 (HMV/K2), and NA138 (HMV/K2).

### Correlation of virulence genes and antibiotic susceptibility

Among HvKp strains, 4 out of 5 (80%) displayed XDR or MDR patterns. Similarly, 82 out of 127 CKp strains (64.6%) showed XDR, MDR, or PDR resistance. These findings are summarized in table 4 (supplementary).

### Discussion

#### Study limitations and key findings

The study encountered several limitations, including difficulties in acquiring isolates, obtaining comprehensive patient information, and assessing the severity of infections.

#### Prevalence of *K. pneumoniae* by clinical specimen

A total of 132 *K. pneumoniae* isolates were recovered from various clinical specimens. Urine was the most common source, followed by respiratory secretions and blood. These results are consistent with findings from previous studies conducted in Iraq (Kadum, 2020; Naqid et al., 2020) and Egypt (Naga, 2021). However, they contrast with other reports (Hassan Mohammed et al., 2020; Maity et al., 2022; Hasib et al., 2023), which suggest differing patterns of distribution based on specimen type. Such variability may be attributed to environmental, socioeconomic, and healthcare-related factors.

#### Antibiotic resistance patterns

Beta-lactams and folic acid synthesis inhibitors demonstrated the highest levels of resistance. The 132 isolates exhibited diverse antibiotic susceptibility profiles, with XDR patterns being most common, followed by MDR and PDR. Non-susceptibility to at least one drug within a specific class was common, although some isolates remained treatable with standard medications.

Our findings align with prior studies (e.g., Hasib et al., 2023), which reported high resistance to ceftazidime and amoxicillin-clavulanate, relative to carbapenems. The predominance of the XDR phenotype is consistent with reports by Al-Baz et al. (2022) and Sharma et al. (2023). While our study found a high prevalence of XDR and PDR isolates, other investigations have documented a higher rate of MDR strains (Farhadi et al., 2021; Jwair et al., 2023; Davoudabadi et al., 2023). These discrepancies likely result from differences in antibiotic stewardship, antimicrobial use, host immunity, infection control measures, and hospitalization frequency.

### Virulence gene analysis

Microviscosity-associated gene A (*magA*), specific to the *K1* serotype and located in the capsular polysaccharide synthesis (*cps*) operon, is a chromosomal gene critical for exopolysaccharide capsule formation. Although it has been strongly linked to pyogenic liver abscesses (83% of cases per Kocsis, 2023), all strains in the present study tested negative for *magA*. Instead, the *K1*-specific gene *wzx\_K1* was used, which targets the same serotype. Among the 132 isolates, 3 (2.3%) were positive for the *wzx\_K1* allele. Interestingly, the *K2* serotype was more prevalent.

Both *K1* and *K2* serotypes exhibit increased resistance to macrophage-mediated clearance, enhancing their virulence. Some virulence genes, such as *rmpA* and *iutA* (aerobactin), contribute to the hypervirulent phenotype, making molecular analysis essential for accurate identification (Shanthini et al., 2023).

In the present study, 4 strains carried *iutA*, and one carried *P-rmpA* without *iutA*. No isolates tested positive for *c-rmpA*, although *P-rmpA* is reportedly more prevalent. Overall, 5 strains (3.8%) were classified as HvKp; the remaining 127 (96.2%) were CKp. HvKp strains were isolated from patients with urinary tract infections, chest infections, and burn wounds.

### Hypermucoviscous phenotype (HMV)

The HMV phenotype, detected via the string test, is a hallmark of hypervirulence. However, it is not exclusive to HvKp. Shanthini et al. (2023) found HMV phenotypes in CKp strains, particularly those with *K1/K2* capsular types. While HvKp often exhibits HMV due to factors such as *magA* and *rmpA*, the absence of these genes in some HMV strains reflects the complexity of hypermucoviscosity.

Our findings, along with those of Osama et al. (2023), suggest that multiple factors—including virulence genes and colonization niches (urinary tract, lungs, gut)—influence HMV and hypervirulence.

### Comparison with previous studies

Saki et al. (2022) found 17 HvKp strains (11.1%) among 153 isolates, with 6 (35.3%) positive for HMV and smaller numbers positive for *magA* and *rmpA*. Vandhana et al. (2022) identified 18 HvKp isolates (13.9%) among 129 strains, 9 of which were HMV-positive. Aerobactin was present in all HvKp strains and was associated with severe infections.

Al-Fahdawi et al. (2023) identified 18 HvKp strains from 100 isolates. Of these, 51% were HMV-positive, and 17 out of 18 HvKp strains showed the HMV phenotype. These studies demonstrate variation in HvKp prevalence and characteristics, consistent with our findings.

### Antibiotic resistance in HvKp vs. CKp

Historically, HvKp strains were considered antibiotic-susceptible, but recent reports indicate a rise in MDR and XDR HvKp due to acquired resistance elements (Kocsis, 2023). MDR-HvKp is capable of spreading in both hospital and community settings, especially among immunocompromised individuals. In contrast, community-acquired HvKp infections in healthy individuals typically involve hypermucoviscous phenotypes and are often mono-microbial.

In this study, 80% of HvKp and 64.6% of CKp strains exhibited MDR, XDR, or PDR resistance patterns. Similar trends have been reported globally (Örsten et al., 2020; Banerjee et al., 2021; Davoudabadi et al., 2023). Resistance in these strains may be attributed to mobile genetic elements, such as IncF1, ColKP3, and IncR plasmids.

### Clinical implications of HvKp infections

HvKp infections are linked to more severe and disseminated disease than CKp infections (Al-Deresawi et al., 2023). Despite the low incidence in this study, the identified HvKp strains exhibited significant resistance, raising concerns about therapeutic challenges.

### Case summaries of HvKp infections

HvKp infections were identified in several cases. Strains NA2 and NA6 were isolated from urine samples of young female outpatients aged 3 months and 10 years, respectively; both exhibited extensively drug-resistant (XDR) profiles, but limited clinical data prevented determination of outcomes or transmission routes. Strains NA105 and NA106, showing multidrug-resistant (MDR) and XDR patterns, were recovered from burn wounds in pediatric patients; however, the absence of detailed patient records restricted further analysis. Strain NA96 was obtained from an endotracheal tube swab of a 32-year-old male with a history of smoking, alcoholism, pancreatitis, and organ failure; this isolate also demonstrated an XDR

profile, and the patient ultimately succumbed to the infection.

### Conclusion

This study provides valuable insights into the prevalence, resistance profiles, and virulence characteristics of *K. pneumoniae* in Iraq. While the incidence of HvKp was relatively low, the strains identified exhibited high resistance levels, emphasizing the need for continuous surveillance and targeted antimicrobial stewardship. The severity of cases associated with HvKp underlines the urgency of developing effective prevention and treatment strategies.

### Funding

Self-funded.

### Conflict of Interest

The author declares no conflict of interest.

### Acknowledgment

The author acknowledges scientific support from the College of Medicine, Al-Nahrain University, and thanks the staff at Ibn Al-Balady Hospital for their assistance.

### Ethical Approval

This study was approved by the Al-Nahrain University College of Medicine Ethics Committee (IRB/192, dated October 14, 2022). Approval was also granted by the Iraqi Ministry of Health and participating hospitals. Patient data were obtained from hospital records; patients were not directly involved.

### References

- Al Jader Z, Ibrahim S. (2022). Molecular detection of pathogenic bacteria (*K. pneumoniae*, *P. aeruginosa*, and *E. coli*) from human saliva. *Microbial Biosystems*, 7(1), 41-51. doi: 10.21608/mb.2022.138972.1058
- Ariyadasa S, Billington C, Shaheen M N F, Ashbolt N J, Fee C J, Pang L. (2022). Use of a Novel DNA-Loaded Alginate-Calcium Carbonate Biopolymer Surrogate to Study the Engulfment of *Legionella pneumophila* by *Acanthamoeba polyphaga* in Water Systems. *Microbiology Spectrum*, 10(4). <https://doi.org/10.1128/spectrum.02210-22>
- Büchle M L C, Nunes B F, Filippin-Monteiro F B, Caumo K S. (2023). Diagnosis and treatment of *Acanthamoeba* Keratitis: A scoping review demonstrating unfavorable outcomes. *Contact Lens and Anterior Eye*, 46(4), 101844. <https://doi.org/10.1016/j.clae.2023.101844>
- Castro A E, Obusan M C. (2023). Microbial quality and emerging pollutants in freshwater systems of Mega Manila, Philippines: A scoping review. *Urban Water Journal*, 20(6), 639–651. <https://doi.org/10.1080/1573062x.2023.2209559>
- Chomicz L, Szaflik J, Baltaza W. (2024). *Acanthamoeba* spp. as factors for severe infectious diseases in humans. MDPI. <https://doi.org/10.3390/microorganisms12030581>
- Fischer A, Anderson D M, Tessmer M H, Frank D W, Feix J B, Meiler J. (2017). Structure and Dynamics of Type III Secretion Effector Protein ExoU As determined by SDSL-EPR Spectroscopy in Conjunction with De Novo Protein Folding. 2(6), 2977–2984. <https://doi.org/10.1021/ACSOMEGA.7B00349>
- Galán J E, Waksman G. (2018). Protein injection machines in bacteria. *Cell*, 172(6), 1306-1318. <https://doi.org/10.1016/j.cell.2018.01.034>
- Hamedo H, El-Morsi A, Hassan A, Badawi E. (2025). In silico synergistic effects of polyhydroxyalkonates with antibiotic resistance profile of *Klebsiella pneumoniae* as promising way in pneumonia treatment. *Microbial Biosystems*, 10(1), 195-205. doi: 10.21608/mb.2025.361987.1258
- Holubova J, Juhasz A, Masin J, Stanek O, Jurnecka D, Osickova A, Sebo P, Osicka R. (2021). Selective Enhancement of the Cell-Permeabilizing Activity of Adenylate Cyclase Toxin Does Not Increase Virulence of *Bordetella pertussis*. *International Journal of Molecular Sciences*, 22(21), 11655. <https://doi.org/10.3390/ijms222111655>
- Horna, G, Ruiz J. (2021). Type 3 secretion system of *Pseudomonas aeruginosa*. *Microbiological Research*, 246, 126719. <https://doi.org/10.1016/j.micres.2021.126719>
- Labovská S. (2021). *Pseudomonas aeruginosa* as a Cause of Nosocomial Infections. In *Pseudomonas aeruginosa - Biofilm Formation, Infections and Treatments*. IntechOpen.
- Leong, W, Poh W H, Williams J, Lutz C, Hoque M M, Poh Y H., et al. (2022). Adaptation to an amoeba host leads to *Pseudomonas aeruginosa* isolates with attenuated virulence. *Applied and Environmental Microbiology*, 88(5). <https://doi.org/10.1128/aem.02322-21>
- Li Y, Sun S X. (2023). The influence of polarized membrane ion carriers and extracellular electrical/pH gradients on cell ionic homeostasis and locomotion. bioRxiv. <https://doi.org/10.1101/2023.07.26.550658>
- Mokabel A, Gebreel H, Youssef H, El-Kattan N, Abdel-Wahhab M. (2024). Prevalence of multidrug resistant bacteria in Egyptian hospitalized patients. *Microbial Biosystems*, 9(2), 121-132. doi: 10.21608/mb.2024.312767.1147

- Milanez G, Masangkay F, Martin I G, Hapan M F, Manahan E, Castillo J, Karanis P. (2022). Epidemiology of free-living amoebae in the Philippines: A review and update. PubMed Central. Retrieved from <https://pmc.ncbi.nlm.nih.gov/articles/PMC9387320>
- Nirjhon R. (2023). BLAST in bioinformatics: Its uses, application & function. Retrieved November 18, 2024, from <https://discover.hubpages.com/education/BLAST2>
- Patil R, Das S, Stanley A, Yadav L, Sudhakar A, Varma A K. (2010). Optimized hydrophobic interactions and hydrogen bonding at the target-ligand interface leads the pathways of drug designing. PLOS <https://doi.org/10.1371/journal.pone.0012029>
- Qin S, Xiao W, Zhuo C, Pu Q, Deng X, Lan L., et al. (2022). *Pseudomonas aeruginosa*: Pathogenesis, virulence factors, antibiotic resistance, interaction with host, technology advances, and emerging therapeutics. Nature Communications. <https://doi.org/10.1038/s41392-022-01056-1>
- Reuven A D, Mwaura B W, Bliska J. (2024). ExoS Effector in *Pseudomonas aeruginosa* Hyperactive Type III Secretion System Mutant Promotes Enhanced Plasma Membrane Rupture in Neutrophils. bioRxiv. <https://doi.org/10.1101/2024.01.24.577040>
- Scruggs B, Quist T, Zimmerman M B, Salinas J, Greiner M. (2024). Risk factors, management, and outcomes of *Acanthamoeba* keratitis: A retrospective analysis of 110 cases. Science Direct. <https://doi.org/10.1016/j.ajoc.2022.101372>
- So-Young K, Aung J M, Shin M, Moon E-K, Kong H-H, Goo Y-K, Chung D-I, Hong Y. (2022). Sirtinol suppresses trophozoites proliferation and encystation of *Acanthamoeba* via inhibition of sirtuin family protein. *The Korean Journal of Parasitology*, 60(1), 1–6. <https://doi.org/10.3347/kjp.2022.60.1.1>
- Springer T I, Reid T-E, Gies S L, Feix J B. (2019). Interactions of the effector ExoU from *Pseudomonas aeruginosa* with shortchain phosphatidylinositides provide insights into ExoU targeting to host membranes. The Journal of biological chemistry. <https://pmc.ncbi.nlm.nih.gov/articles/PMC6916483/>
- Teixeira-Nunes M, Retailleau P, Raoux-Barbot D, Comisso M, Missinou A A, Velours C., et al. (2023). Functional and structural insights into the multi-step activation and catalytic mechanism of bacterial ExoY nucleotidyl cyclase toxins bound to actin-profilin. bioRxiv. <https://doi.org/10.1101/2023.01.13.523968>
- Tessmer M H, DeCero S A, del Alamo D, Riegert M O, Meiler J, Meiler J, Frank D W, Feix J B. (2020). Characterization of the ExoU activation mechanism using EPR and integrative modeling. Scientific Reports, 10(1), 19700. <https://doi.org/10.1038/S41598-020-76023-3>
- Wang X, Parashar K, Sitaram A, Bliska J B. (2014). The GAP activity of type III effector YopE triggers killing of *Yersinia* in macrophages. PLOS Pathogens, 10(8). <https://doi.org/10.1371/JOURNAL.PPAT.1004346>
- Wang Y, Jiang L, Zhao Y, Ju X, Wang L, Jin L, Fine R D, Li M. (2023). Biological characteristics and pathogenicity of acanthamoeba. *Frontiers in Microbiology*, 14. <https://doi.org/10.3389/fmicb.2023.1147077>
- Zhang X, Yu C-X, Song L-J (2024). Progress on the Regulation of the Host Immune Response by Parasite-Derived Exosomes. Pathogens, 13(8), 623. <https://doi.org/10.3390/pathogens13080623>